

New diagnostic estimates of variations in terrestrial water storage based on ERA-Interim data

Brigitte Mueller,* Martin Hirschi and Sonia I. Seneviratne*

Institute for Atmospheric and Climate Science, Swiss Federal Institute of Technology (ETH), Zürich, Switzerland

Abstract:

Terrestrial water storage is an important component of the climate system as it determines the partitioning of the water and energy fluxes at the land surface. Since *in situ* measurements are scarce, there is a strong need for alternative validation data sources.

Here we present a new dataset of monthly basin-scale terrestrial water storage changes (TWSC) derived with the combined atmospheric-terrestrial water-balance approach, also referred to as basin-scale water-balance (BSWB) approach. It is diagnosed from observation-constrained reanalysis data for the atmospheric fields and observed streamflow. A previous BSWB dataset derived from the European Center for Medium-Range Weather Forecasts (ECMWF) reanalysis ERA-40 provided reasonable estimates of TWSC for mid-latitude basins. The here presented BSWB dataset is derived from the latest ECMWF reanalysis ERA-Interim, which is available in real time. The potential real-time availability of TWSC derived from ERA-Interim is of great relevance for several agricultural, hydrological, and climate applications.

An uncertainty analysis of the derived TWSC highlights the importance of the atmospheric moisture flux convergence fields from the reanalysis for the resulting product uncertainty. We find that the BSWB estimates have a relative uncertainty of about 4–6% in basins larger than 1.5×10^6 km² compared with the mean seasonal cycle. The ERA-Interim based dataset compares better with *in situ* soil moisture, snow depth, and groundwater measurements in the Ob basin and Illinois than the previous ERA-40 based dataset. We further compare the BSWB datasets to retrievals from the Gravity Recovery And Climate Experiment (GRACE), scatterometer data from the European Remote Sensing (ERS) satellites, and land surface model output from the second phase of the Global Soil Wetness Project (GSWP). We find a better correlation between ERS and the BSWB data than between GRACE and the BSWB data, which might be related to the relatively coarse resolution of GRACE. GSWP model output and the BSWB datasets compare well in most of the studied river basins. Copyright © 2010 John Wiley & Sons, Ltd.

KEY WORDS terrestrial water storage; water-balance; ERA-Interim

Received 26 September 2009; Accepted 3 February 2010

INTRODUCTION

Soil moisture is a key variable of the climate system (e.g. Seneviratne *et al.* 2010). Nevertheless, there is a lack of *in situ* soil moisture observations in most regions in the world. Where available, soil moisture observations often cover relatively short time periods, and can thus not be used to study decadal variations. Moreover, *in situ* measurements are point-scale observations and are not representative for larger areas. Therefore, techniques such as satellite remote sensing (see e.g. McCabe *et al.* 2008, de Jeu *et al.* 2008), and the combined atmospheric-terrestrial water-balance approach (e.g. Seneviratne *et al.* 2004, Hirschi *et al.* 2006a,b) have been used to obtain information on terrestrial water storage (TWS). The main components of TWS are soil moisture, snow, groundwater, and surface water (and in some regions ice cover).

Previous studies from Seneviratne *et al.* (2004) and Hirschi *et al.* (2006a, 2007) have resulted in the creation of the basin-scale water-balance (BSWB) dataset,

which includes atmospheric-terrestrial water-balance estimates of terrestrial water storage changes (TWSC) for several river basins of the world (downloadable from www.iac.ethz.ch/data/water_balance/). The advantage of the BSWB approach is its long-term coverage: It is based on atmospheric data from reanalysis products and streamflow measurements, which are both available over several decades. The validation of this approach for Illinois (Seneviratne *et al.* 2004) and several major river basins in the mid-latitudes (Hirschi *et al.* 2006a) reveals good agreement with observations. The method has been shown to be valid on a scale of roughly 10⁵ km² and above (Rasmusson 1968, Seneviratne *et al.* 2004, Hirschi *et al.* 2006a). The previously derived estimates, hereafter referred to as E40-BSWB, were based on ERA-40 reanalysis data from the ECMWF for the atmospheric water vapour fields, thus limiting the dataset to the ERA-40 period (1958–2002). Note that estimates based on the ECMWF operational analysis data were also more recently derived for some applications (Andersen *et al.* 2005, Hirschi *et al.* 2006b).

The dataset presented in this study, hereafter referred to as EI-BSWB, is based on the latest ECMWF reanalysis data product ERA-Interim (www.ecmwf.int/research/era/

* Correspondence to: Brigitte Mueller and Sonia I. Seneviratne, Institute for Atmospheric and Climate Science, Swiss Federal Institute of Technology (ETH), Zürich, Switzerland.
E-mail: brigitte.mueller@env.ethz.ch; sonia.seneviratne@env.ethz.ch

do/get/era-interim). Compared with ERA-40, ERA-Interim is characterized by a higher resolution and improvements in the humidity analysis, which is of advantage for the accuracy of the derived TWSC estimates. Moreover, the ERA-Interim reanalysis is available in real time, which is crucial for several applications. EI-BSWB estimates could thus provide near real-time information on TWSC even in regions where no soil moisture, precipitation, or evaporation measurements are available. A similar real-time application was recently tested for the Colorado river basin with atmospheric data from the North American Regional Reanalysis (NARR, Troch *et al.* 2007, <http://voda.hwr.arizona.edu/twsc/sahra>). Since deep water impacts hydrology and climate through root water uptake as well as a prolonged land water memory (Kleidon and Heimann 2000, Koster *et al.* 2004, Seneviratne *et al.* 2006a,b, Zeng *et al.* 2008), both the BSWB and GRACE datasets have the asset of providing whole TWS information, rather than only soil moisture. Furthermore, knowledge on changes in groundwater storage is crucial for several countries (e.g. Rodell *et al.* 2009). The large-scale and long-term availability of the dataset is an advantage for the quantification of the water cycle, detection of droughts, and validation of climate and hydrological models.

This study is the first to assess the accuracy of the BSWB estimates. In addition, the performance of the ERA-Interim based estimates is compared with that of the ERA-40 based estimates. Finally, we compare the EI-BSWB dataset to TWS estimates from ground observations, two remote sensing products (scatterometer data from the European Remote Sensing (ERS) satellites and GRACE retrievals), as well as land surface model output (GSWP-2 data).

METHODS AND DATA

Basin-scale water-balance dataset

Combined atmospheric and terrestrial water-balance approach. The BSWB estimates of TWSC are obtained from the combined terrestrial and atmospheric water-balance approach, which has been proposed by e.g. Rasmusson (1968) and recently employed by e.g. Masuda *et al.* (2001), Seneviratne *et al.* (2004) and Hirschi *et al.* (2006a,b). TWSC ($\partial S/\partial t$) can be computed from the column storage of water vapour (W), the vertically integrated water vapour flux (\bar{Q}), and streamflow (R) using

$$\left\{ \frac{\partial S}{\partial t} \right\} = - \left\{ \frac{\partial W}{\partial t} \right\} - \overline{\nabla_H \cdot \bar{Q}} - \{\bar{R}\}, \quad (1)$$

where ∇_H denotes the horizontal divergence, the overbar a temporal average and $\{\}$ an areal average (over a river basin). General discussions of the limitations of the combined atmospheric-terrestrial water-balance approach are provided by Rasmusson (1968), Seneviratne *et al.*

(2004) and Hirschi *et al.* (2006a). In particular, several studies have shown that Equation (1) is only valid on a scale of 10^5 – 10^6 km², because $-\nabla_H \cdot \bar{Q}$ from climate models or reanalysis can be quite erratic for smaller basins (e.g. Yeh *et al.* 1998, Berbery and Rasmusson 1999, Seneviratne *et al.* 2004).

The previously derived BSWB estimates have been validated with ground observations in several regions (Seneviratne *et al.* 2004, Hirschi *et al.* 2006a) and have been used in numerous applications (e. g. Rodell *et al.* 2004, Andersen *et al.* 2005, Syed *et al.* 2005, Seneviratne *et al.* 2006a, Hirschi *et al.* 2007, Balsamo *et al.* 2009, Jaeger *et al.* 2009).

Data sources. The convergence of the vertically integrated water vapour flux ($-\nabla_H \cdot \bar{Q}$) and the changes in atmospheric moisture content ($\partial W/\partial t$) used in Equation (1) are derived from reanalysis data. These fields are assumed to be of high quality since they are strongly constrained by the assimilation of radiosonde data in the reanalysis data product. However, this means also that the quality may be dependent on the density of the radiosonde data in the respective regions. Previous studies were based on the ERA-40 reanalysis (Seneviratne *et al.* 2004, Hirschi *et al.* 2006a) and the ECMWF operational analysis (Andersen *et al.* 2005, Hirschi *et al.* 2006b). Here we use the newest ECMWF reanalysis data product ERA-Interim. The moisture flux divergence is calculated on a spectral space instead of pressure level fields, in order to maintain maximum resolution during the calculation (for a detailed description see Seneviratne *et al.* 2004).

The previously used ERA-40 reanalysis has known issues in its representation of the hydrological cycle. In particular, it exhibits physically unrealistic results over the tropics and subtropics; in the monsoon trough and convergence zones, precipitation is overestimated, and the values of evaporation minus precipitation are too low (Uppala *et al.* 2005, Trenberth *et al.* 2007). In the subtropics, evaporation over land is overestimated. The ERA-40 assimilation includes different radiance data which are used to correct a too dry model state in non-precipitating regions over the tropical ocean. In an analysis-assimilation feedback loop, it led to excessive precipitation over the tropical ocean (see Simmons *et al.* 2007). Many of these issues have been addressed in the new ERA-Interim reanalysis. In particular, it includes a new humidity analysis and improved model physics, changes in the radiance assimilation, and variable bias corrections. In a preliminary analysis of the performance of ERA-Interim, Simmons *et al.* (2007) found an improvement in the total column water vapour fields. Further changes implemented in the new ECMWF reanalysis include: (1) a 12-h 4D-Var assimilation technique (ERA-40 3D-Var), (2) a higher horizontal resolution (T255 vs T159, corresponding to grid-spacings of about 80 km for ERA-Interim and 110 km for ERA-40), and (3) improved data quality

control (see also www.ecmwf.int/research/era/do/get/era-interim). Moreover, the ERA-Interim reanalysis is available in near real time.

For the streamflow data used in Equation (1), we assume that groundwater runoff is included and human water removal is negligible. River streamflow data has been obtained from many different institutions (see Acknowledgements). The catchment definitions of the investigated river basins were derived from the HYDRO1k dataset, as described by Hirschi *et al.* (2006a).

Drift correction. In the long term, the water input to a basin should be balanced by the water output, i.e. the storage remains constant. This assumption is generally correct for multi-year means, although some regions may show persistent trends, due for instance to groundwater withdrawal (Rodell *et al.* 2009). Since the changes in column storage of water vapour are negligible for annual to long-term means, the water input is defined through the vertically integrated water vapour flux ($-\nabla_H \cdot \bar{Q}$ in Equation (1)). The difference between the long-term means of the vertically integrated water vapour flux and the streamflow of a river basin is referred to as imbalance (*Imb*) and can be computed from the temporal integration of the derived TWS variations

$$Imb = \int_{t_0}^t \left\{ \frac{\partial \bar{S}}{\partial t} \right\} dt, \quad (2)$$

that should equal zero when averaged over several years (with the exception of regions with long-term trends in TWS). Long-term deviations, i.e. imbalances ($Imb \neq 0$) occur due to the accumulation of small errors over time. These imbalances are a measure of the agreement between the atmospheric and hydrological data used in the combined water balance. As suggested by Seneviratne *et al.* (2004), the most likely causes for the imbalances are systematic biases in the atmospheric moisture flux convergence of the employed reanalysis dataset, since streamflow errors are small (see below) and the total column storage of water vapour does not contribute significantly to the derived TWSC in the long term. Hirschi *et al.* (2006a) suggested to use a simple high-pass filter (subtraction of 3-year running mean) to remove the drift of dS/dt successfully. This filter is also applied here.

Sources and estimation of uncertainty of derived TWSC estimates. Since total column water vapour is a comparably small contributor to TWS in Equation (1), the two main sources of uncertainty arise from the reanalysis' divergence of water vapour flux and the measured streamflow. We assume here that streamflow is measured with an accuracy of 10% (which was found in 70% of daily runoff records studied by Gutowski *et al.* 1997). To obtain an estimate of the uncertainty in the water vapour flux convergence, we use mean monthly absolute differences between (1) ERA-Interim and ERA-40, and (2) ERA-Interim reanalysis and ERA-Interim 6-h forecast. Another measure of the uncertainty in the derived TWSC are the accumulated imbalances described in Equation (2).

Comparison datasets

We use here several alternative datasets of TWSC for comparison with the newly derived EI-BSWB estimates. An overview of all considered datasets can be found in Table I.

In situ measurements. The comparison of the EI-BSWB dataset with *in situ* measurements is performed for areas where the period of available data is overlapping, i.e. for the Ob river basin and Illinois. The *in situ* soil moisture measurements used in the present study are obtained from the Global Soil Moisture Data Bank (Ob basin and Illinois, Robock *et al.* 2000). Snow depth observations in the Ob basin originate from the Historical Soviet Daily Snow Depth - Version 2.0 (obtained from the National Snow and Ice Data Center, Boulder, USA) and in Illinois from the Midwest Regional Climate Center (MRCC; available at <http://mrcc.sws.uiuc.edu>). The snow depth is converted into water equivalents using a constant density value of 100 kg m^{-3} . Groundwater measurements are only available for Illinois (from the Illinois water and climate summary Water and Atmospheric Resource Monitoring (WARM) Program; for a detailed description of the groundwater change computation, see Seneviratne *et al.* 2004).

E40-BSWB. The E40-BSWB dataset has already been validated in previous studies by Seneviratne *et al.* 2004

Table I. Overview of used TWS datasets

Dataset	Spatial resolution	Description	Temporal coverage
EI-BSWB	300–1000 km	Whole terrestrial water storage	1989–2008, but depending on streamflow data availability
E40-BSWB	300–1000 km	Whole terrestrial water storage	1958–2002, but depending on streamflow data availability
ERS SWI	25 km	SWI (100 cm)	1992–2000 full global coverage 2003–2006 partial coverage
GRACE	500 km	Whole terrestrial water storage	2002–2008
GSWP	110 km	Whole terrestrial water storage	1986–1995
<i>in situ</i> measurements Ob	Point measurements	Soil moisture and snow depth	1990–1995 soil moisture and snow 1996–1998 soil moisture
<i>in situ</i> measurements Illinois	Point measurements	Soil moisture, groundwater and snow	1990–2000

(for Illinois) and Hirschi *et al.* 2006a (for the Volga, Ob, Dnepr and Don basins). We use here this dataset for a comparison to the EI-BSWB data, as well as to some of the other considered datasets (ground observations, remote sensing data and model output, depending on the time period available). Improvements from E40- to EI-BSWB data are expected, given the improvements in the reanalysis see 'Basin-scale water-balance dataset'.

ERS scatterometer estimates. We compare the derived EI-BSWB dataset to the Soil Water Index (SWI) processed at the Institute of Photogrammetry and Remote Sensing, Vienna University of Technology (Austria, TU Wien, www.ipf.tuwien.ac.at/radar/ers-scat/home.htm), which is based on measurements from the scatterometers onboard the ERS Satellites ERS-1 and ERS-2. The radiation reflected by the surface depends on the water content of the soil, but also on vegetation and surface roughness. To account for these confounding effects, a change of detection approach is applied (Scipal *et al.* 2002). The computation of the SWI, which represents the soil moisture content in the top 1 m of the soil in relative units ranging between the wilting point and field capacity, involves a two-layer infiltration model. SWI data are available from 1991 to present, with global coverage until 2001. The horizontal resolution of the measurements is 25 km.

Despite the involved uncertainties, Wagner *et al.* (2003) showed that overall, ERS and modelled soil moisture agree well. However, the performance of scatterometer data is limited in densely vegetated areas, deserts, and mountainous regions (de Jeu *et al.* 2008).

GRACE TWS retrievals. The GRACE twin satellites have been measuring changes in the Earth's gravity field with high accuracy since March 2002. These gravity measurements are used to derive TWSC datasets at three centres: CSR (University of Texas, Center for Space Research), GFZ (GeoForschungsZentrum, Potsdam), and JPL (Jet Propulsion Laboratory, California Institute of Technology). We herein analyse the release 2004 from the CSR, since a comparison of the present products of the three data centres displays little differences (not shown). Note that this was not the case for previous releases (Hirschi *et al.* 2006b). Comparing the release 2004 to previous releases, the implemented changes include improved background geophysical models and data processing techniques (Betadpur 2007). We used here data with a smoothing radius of 500 km (half-width of the equivalent gaussian smoother). The data are available from April 2002 to present (downloadable from the Tellus website <http://podaac.jpl.nasa.gov>).

Similar to the ERS derived estimates, GRACE observations have to undergo retrieval algorithms, which are associated with errors and uncertainties. Several studies have found reasonable agreement of hydrological variables from GRACE and model output or observations. For instance Swenson *et al.* (2006) compared TWSC

from GRACE with *in situ* measurements in Illinois. They showed that accurate estimates from GRACE can be obtained on a spatial scale of roughly 300 km. Yamamoto *et al.* (2007), studying four major river basins of the Indochina peninsula using GRACE and model simulation data, found that the agreement between the two datasets is good in the two larger basins studied, whereas the agreement is poorer in the smaller basins. This finding is related to the smoothing radius, which has to be applied in order to suppress higher degree errors. A small smoothing radius is beneficial for detecting fine spatial scale mass variations, but on the other hand suffers from measurement errors at higher degrees. Awange *et al.* (2009), who compared GRACE data with observations over Australia, noted that while major signals could be detected in this region, there were still deficiencies in the standard GRACE data processing and filtering methods, leading to problems when studying basins with a small amount of water. On the other hand, Rodell *et al.* (2009) showed that GRACE captures a strong signal of TWSC in north-western India, which is consistent with reports of groundwater withdrawal in this area. Thus overall it appears that GRACE can provide useful information though some uncertainties remain (see also Ramillien *et al.* 2008).

GSWP. We further compare the EI-BSWB dataset to the multi-model output from the second phase of the Global Soil Wetness Project (GSWP, Dirmeyer *et al.* 2006). A total of 12 land surface models participated in the second phase of the GSWP and provided simulations over the 1986–1995 time period. The multi-model average was found to be generally as good as or better than the best of the contributing models (Guo *et al.* 2007).

In our comparison, we include the changes in column soil moisture, snow-water equivalent, surface liquid water storage, and canopy interception in the GSWP TWSC fields, in order to include as many of the TWS components as possible. Note that they do generally not include groundwater changes due to model structure.

Data processing. The *in situ* measurements of soil moisture, snow depth and groundwater, GRACE satellites retrievals, SWI from the ERS scatterometer data, and model output are individually independent datasets that can be compared to the BSWB data. The comparison is done on the river basin scale (for the corresponding map see Figure 1). For the *in situ* data, all stations available in the Ob basin and Illinois area, respectively, are averaged with equal weight. The GRACE, ERS and model output data are averaged over the basins using the catchment definitions described in 'Data sources'. When comparing to absolute values, the monthly TWSC from the BSWB approach are integrated.

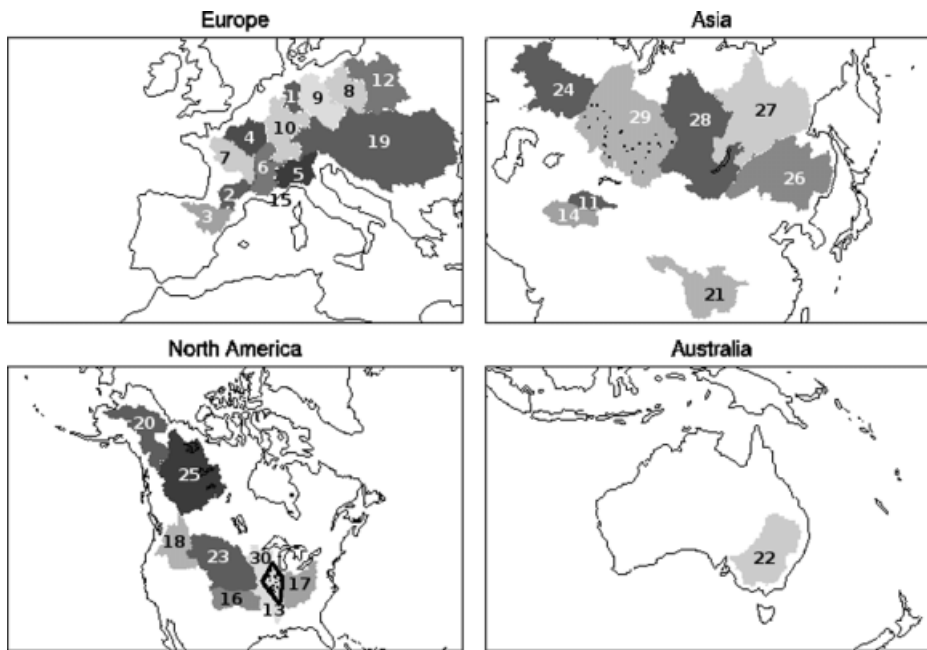


Figure 1. River basins considered, for legend see Table III. Note that No. 15 (French basins) includes the basins No. 2, 4, 6 and 7. The dots in the basins No. 29 (Ob) and No. 13 (Illinois) denote the soil moisture observations considered in this study. The BSWB TWS data in the Illinois area is derived on quadrilaterals (shown) to assure a good accordance with observations

RESULTS AND DISCUSSION

EI-BSWB dataset and its uncertainties

In order to assess the validity of the EI-BSWB TWSC, we evaluate here the uncertainty sources for these estimates. In Table II, different uncertainty estimations for the single components of the EI-BSWB TWS data are provided. We use two different approaches to estimate the total uncertainty in the EI-BSWB data: (1) We estimate the uncertainty as the sum of the uncertainties of streamflow and moisture convergence which are computed as described in 'Methods and data', and (2) the imbalances over the considered years (1991–2001) between the atmospheric and terrestrial data are used as an uncertainty estimate.

For the first approach, the uncertainty estimates of moisture convergence are calculated from the differences of ERA-Interim and ERA-40 as well as from the differences of ERA-Interim reanalysis and ERA-Interim 6-h forecast data. Note that when using the two reanalyses, improvements from the ERA-40 to the ERA-Interim reanalysis may lead to an overestimation of the uncertainty for the EI-BSWB estimates. The differences between the ERA-Interim reanalysis and 6-h forecast data are the increments of the reanalysis, i.e. the systematic errors of the model. These increments are only meaningful in regions with sufficient observations (e.g. Fitzmaurice and Bras 2008).

To obtain the relative uncertainties, the absolute total uncertainties (moisture convergence and streamflow uncertainty) are divided by the amplitudes of the derived TWS cycles, i.e. the absolute difference of the maximum and minimum TWS values within the mean seasonal cycle. The standard deviation of the monthly values of the TWS series is also provided in Table II. The river basins

are ordered in ascending size, because the quality of the BSWB estimates has been shown to be closely related to the size of the basins under consideration (Hirschi *et al.* 2006a).

Comparing the estimated uncertainties of streamflow with the total estimated uncertainty obtained from the differences in moisture convergence, it is evident that the uncertainty of the streamflow measurements contributes only little to the total uncertainty. When using the moisture convergence differences between ERA-Interim and ERA-40, the streamflow accounts for less than 20% of the total estimated uncertainty in 16 and, when using ERA-Interim reanalysis and ERA-Interim 6-h forecast differences, in 10 out of the 24 investigated basins. Only in the Lena basins (ERA-Interim/ERA-40 difference) and the Yenisei and Ob basin (ERA-Interim reanalysis/6-h forecast difference) the streamflow uncertainty accounts for more than 50% of the total uncertainty. Consequently, the uncertainty of the moisture convergence is the main contributor to the total uncertainty. Previous studies (e.g. Gutowski *et al.* 1997) suggested that streamflow is measured with good accuracy, and therefore the imbalances between streamflow and moisture convergence, which are seen as an uncertainty estimate of the BSWB data, arise from small systematic errors in the moisture convergence of the employed reanalysis data (Seneviratne *et al.* 2004). This assumption is supported by our results. The uncertainties of the moisture flux convergences (and the related total estimated uncertainties) show a strong decreasing tendency towards large basin sizes. The relative estimated uncertainties also decrease with increasing basin size and amount to less than 10% for the largest river basins under study (roughly larger than 10^6 km²). Note that the uncertainties estimated from the ERA-Interim reanalysis-

Table II. Estimates of uncertainty of the EI-BSWB dataset (1991–2001). Basins, for which the dataset does not cover the period 1991–2001, are omitted from this analysis: Odra, Syrdarya, Wisla, Danube, Mackenzie and Mississippi

	Est. streams-flow uncertainty [mm/d]	Moist. convergence difference EI-E40 [mm/d]	Moist. convergence difference EI-FC [mm/d]	Total est. uncertainty (E40-EI+sf.) [mm/d]	Relative est. uncertainty (E40-EI+sf.) [%]	Total est. uncertainty (EI-FC+sf.) [mm/d]	Relative est. uncertainty (EI-FC+sf.) [%]	Est. uncertainty (imbalance) [mm/d]	Relative est. uncertainty (imbalance) [%]	Mean amplitude TWS [mm/d]	Stdev TWSC [mm/d]	Basin size [km ²]
1	Weser	0.08	0.77	0.85	36.7	0.45	19.7	-0.38	16.6	2.31	1.16	35888
2	Garonne	0.11	0.78	0.88	26.9	0.52	15.7	-0.52	15.7	3.28	1.35	49381
3	Ebro	0.03	0.92	0.95	31.2	0.48	15.9	-0.43	14.1	3.03	1.15	83930
4	Seine	0.07	0.81	0.88	24.8	0.52	14.8	-0.09	2.6	3.53	1.64	84144
5	Po	0.18	0.73	0.91	42.6	0.86	40.3	-0.59	27.4	2.13	1.34	85223
6	Rhone	0.16	0.79	0.95	30.2	0.75	23.7	-0.65	20.7	3.14	1.52	94836
7	Loire	0.07	0.77	0.84	30.7	0.39	14.5	-0.20	7.4	2.73	1.23	107646
9	Elbe	0.04	1.13	1.17	52.7	0.36	16.3	-0.23	10.3	2.22	0.99	132014
10	Rhine	0.13	0.60	0.72	27.4	0.42	15.7	-0.39	14.8	2.64	1.22	160704
13	Illinois	0.02	0.64	0.66	21.8	0.51	16.7	0.26	8.6	3.03	1.45	203549
14	Amudarya	0.04	0.42	0.46	11.5	0.36	8.9	0.07	1.7	3.99	1.50	321599
15	French b.	0.10	0.54	0.64	20.8	0.38	12.4	-0.32	10.5	3.06	1.34	336007
16	Arkansas	0.03	0.63	0.66	34.7	0.43	22.9	-0.19	10.0	1.89	0.98	382423
17	Ohio	0.14	0.48	0.62	27.0	0.46	20.0	-0.52	22.4	2.30	1.12	503558
18	Columbia	0.07	0.56	0.63	14.8	0.19	4.4	0.04	1.0	4.26	1.66	600730
20	Yukon	0.08	0.13	0.20	8.3	0.17	6.9	0.02	0.9	2.45	0.84	779081
21	Changjiang	0.12	0.29	0.41	16.8	0.46	18.9	0.17	7.1	2.43	0.87	965180
22	Murray-D.	0.00	0.29	0.29	24.2	0.26	22.0	-0.49	40.5	1.20	0.70	1006173
23	Missouri	0.01	0.25	0.26	12.6	0.18	8.6	0.09	4.2	2.08	0.90	1201513
24	Volga	0.05	0.13	0.18	6.3	0.12	4.2	-0.05	1.6	2.87	1.16	1333747
26	Amur	0.03	0.11	0.14	6.2	0.12	5.1	-0.02	0.9	2.32	0.78	1921624
27	Lena	0.06	0.05	0.11	4.1	0.10	3.6	-0.09	3.3	2.76	0.89	2351052
28	Yenisei	0.07	0.07	0.14	4.5	0.10	3.3	-0.13	4.2	3.05	0.92	2513361
29	Ob	0.04	0.07	0.11	4.0	0.08	2.8	-0.04	1.3	2.75	0.95	2859889

FC, ERA-Interim 6-h forecast; sf., streamflow; Est., estimated; and Moist., moisture

forecast values tend to be smaller than when estimated from the difference between ERA-Interim and ERA-40. This could point to an overestimation of the uncertainty with the latter approach, in particular in the cases where significant improvements can be expected between ERA-Interim and ERA-40 (i.e. the differences are not random).

The imbalances between cumulative streamflow and moisture convergence show very large variations between the different basins: The smallest values are around 0.02 mm/d (Amur, Yukon), but values of up to more than 0.5 mm/d also occur (Garonne, Rhone, Ohio, Po). The imbalances are clearly smaller for large basins than for small basins. Exceptions are the Seine and Amudarya basins, which exhibit small imbalances (0.09 and 0.07 mm/d) despite their relatively small sizes. On the other side of the range are the Yenisei, Murray-Darling and Ohio basins with anomalously large imbalances (0.13, -0.49 and -0.52 mm/d, respectively). In all river basins except for the Murray-Darling river basin, the relative and absolute imbalances are smaller than the estimated uncertainties from the differences in moisture convergence from ERA-Interim and ERA-40 and streamflow uncertainties. The semi-arid Murray-Darling basin is characterized by very small absolute monthly values of moisture convergence. This could lead to an underestimation of the uncertainty when comparing the monthly ERA-Interim with ERA-40 moisture convergences. The higher imbalance reflects a more realistic estimate of the accuracy in the Murray-Darling basin. Also Draper and Mills (2008) found that the water budget of the Murray-Darling basin could not be confidently estimated with both a model and two reanalysis data products, most likely due to the spatial coverage of the atmospheric moisture soundings. In addition, part of the unusually high negative imbalance (given its large size) could also be explained by a real decrease in TWS in this region (such as is the case in other regions, e.g. Rodell *et al.* 2009), but cannot be evaluated with the BSWB method. The uncertainty estimates from the moisture convergence of ERA-Interim reanalysis and ERA-Interim 6-h forecast also show larger values than those from the imbalances in most basins: Only the Murray-Darling, Ohio and Yenisei basins reveal smaller uncertainties when using the imbalances than the moisture convergence and streamflow errors.

The imbalances (long-term drifts) are negative in most river basins (18 out of the 24 basins). This most likely results from an underestimation of water vapour convergence in the ECMWF reanalyses, as suggested by Hirschi *et al.* (2006a). Positive imbalances are found in the Changjiang, Illinois, Columbia, Missouri, Yukon and Amudarya basins. This could be linked to human influence and therefore streamflow underestimation, or real changes in the water balance in these regions: The Changjiang streamflow for example is measured at the three gorges dam; the Columbia, Missouri, and Yukon basins include areas with strong agricultural activity.

Comparison between EI-BSWB and E40-BSWB

In the following, the EI-BSWB TWSC are compared to the previously derived and validated E40-BSWB estimates. Figure 2 shows the dependence of the imbalances of the EI- and E40-BSWB datasets on the basin size for the common period 1991–2001. Imbalances from the EI-BSWB are displayed in black, those from ERA-40 in red. Different regions are indicated with specific symbols (see legend). This analysis shows a clear tendency of decreasing imbalances with increasing basin size (see also previous section and Hirschi *et al.* 2006a). Comparing the EI- and E40-BSWB datasets, it is worth noting that the large basins in Russia and China have small imbalances in both datasets, with only minor changes from the previous to the present reanalysis. The Murray-Darling as well as the Missouri river basins exhibit smaller imbalances for the EI-BSWB than for the E40-BSWB estimates, which might indicate slight improvements in the moisture convergence data over these areas. Interestingly, the imbalances of 5 out of 16 basins change from a positive (E40) to a negative (EI) sign, while 10 remain unchanged, and only one changes from negative to positive.

Figure 3, top left panel, displays the correlation between the EI-BSWB and E40-BSWB data. Owing to the strong seasonality of TWS, the correlation for the monthly anomalies relative to the mean seasonal cycle (calculated based on a temporal identical sample population) are shown. The number of mutual observations is provided in Table III. The correlations vary strongly between the basins under consideration. Highest values ranging from 0.9 to 0.96 are observed in the Russian basins Yenisei, Lena, Ob, Volga, as well as in the Mackenzie basin. Most small basins show an average correlation of between 0.7 and 0.8. The correlations in the smallest basins are around 0.6 and less.

Validation with observations

In Figure 4, scatter plots for EI-BSWB TWSC versus *in situ* observations in the Ob basin and in Illinois

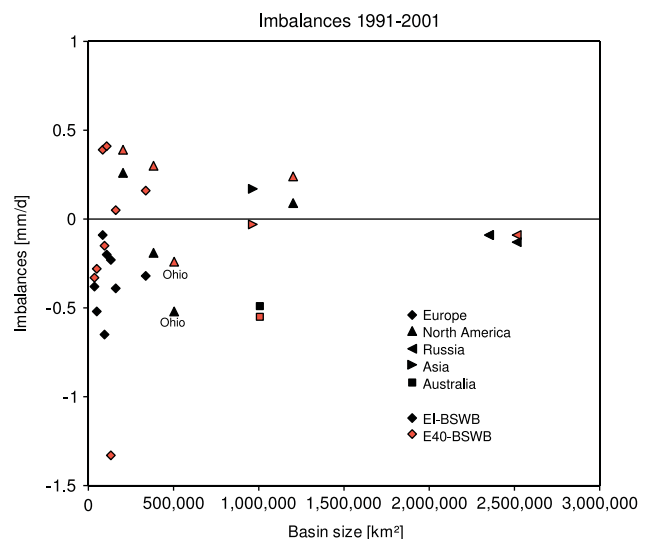


Figure 2. EI- (black) and E40-BSWB (red) TWS imbalances versus basin size. The imbalances are representative for the period 1991–2001

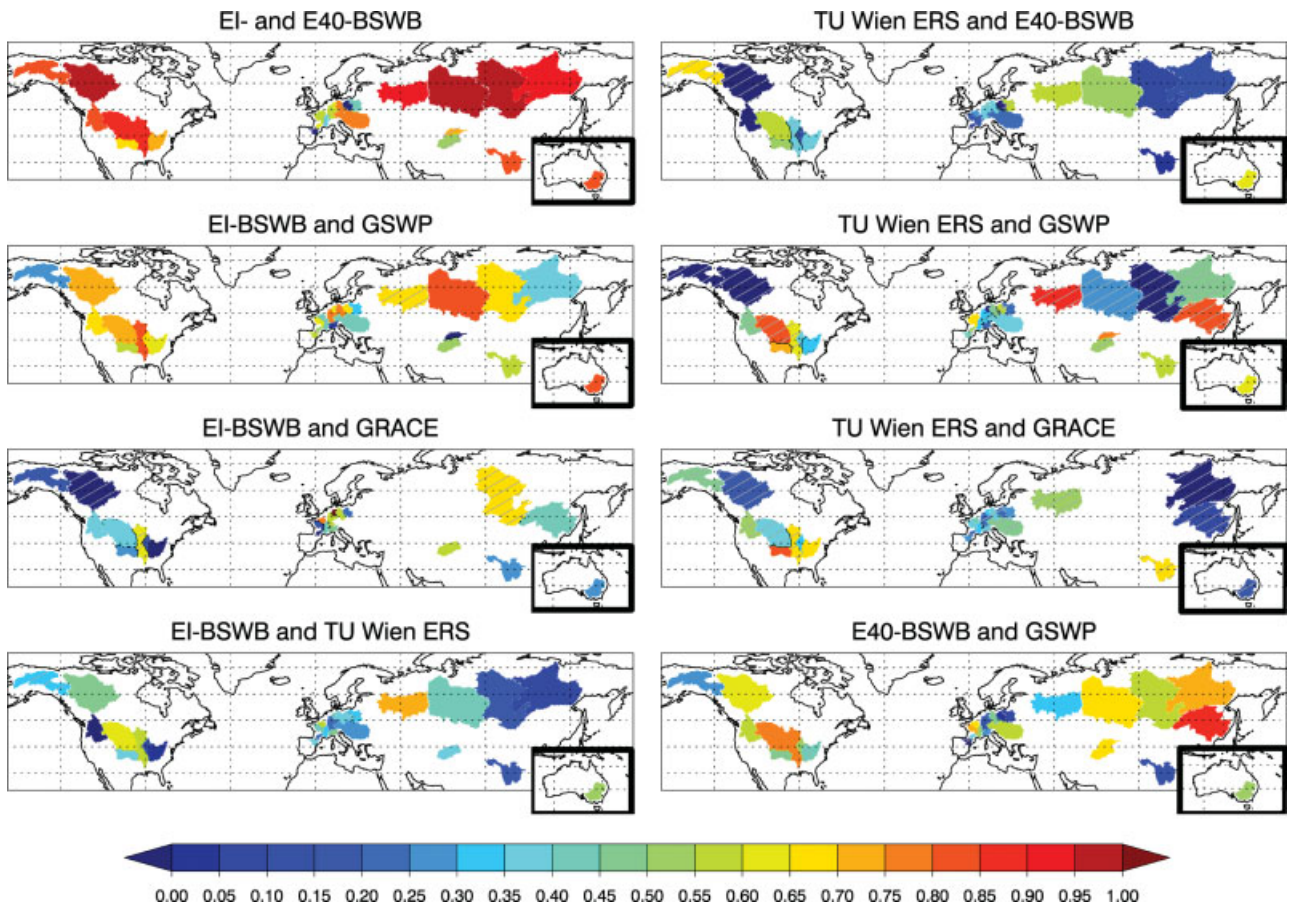


Figure 3. Correlation of monthly anomalies of EI-, E40-BSWB, GRACE and GSWP TWSC and TU Wien ERS SWI estimates. For the number of observations, on which the correlations are calculated, see Table III. Basins where the correlations are based on less than 30 observations are hatched in grey. Inlets of Australia are not to scale

are shown for the period 1990–1995, and 1990–2000, respectively. The upper graphs display the correlation of the monthly absolute TWSC, whereas the lower graphs show the correlation of its monthly anomalies (with removed seasonal cycle). The correlation of the monthly TWSC is highly significant with values of 0.72 (Ob) and 0.82 (Illinois), respectively. The slope in the Ob basin (1.74) shows that the BSWB data overestimate the observed changes (including soil moisture and snow depth only) slightly. The opposite is true for Illinois: The slope of 0.68 indicates an underestimation of observations. The correlation of the monthly anomalies (lower graphs) amounts to 0.43 (Ob) and 0.73 (Illinois), respectively.

These results show that TWSC can be successfully derived with the BSWB approach using the present ECMWF reanalysis ERA-Interim. The good correlation with the previously derived E40-BSWB data (see previous section), and the good comparability of the latter with *in situ* observations in additional basins and regions (Seneviratne *et al.* 2004, Hirschi *et al.* 2006a) further strengthen this finding. An evaluation of EI-BSWB versus E40-BSWB and GSWP for these two regions is presented in the following section (see also Figure 7).

Comparison with GRACE satellites retrievals, ERS SWI, and GSWP model output

The GRACE satellites provide TWSC estimates, which are therefore directly comparable to the BSWB TWS data. In the case of the GSWP data, also the whole TWSC from the models are considered, though these do generally not include groundwater changes due to model structure. Figure 5 shows the mean annual amplitudes of TWS from EI- and E40-BSWB data, GRACE and GSWP TWS. All available years are considered. The comparison shows a generally good agreement of the BSWB datasets with the GRACE and GSWP data in smaller (upper graph) and larger basins (lower graph), with the exception of the Yukon and Volga basins, where GRACE and GSWP show much larger amplitudes than the BSWB data.

As an example, Figure 6 displays time series of EI-BSWB and GRACE TWS for the Seine and Murray-Darling basins. The EI-BSWB TWS data (black lines) cover the entire period shown (1992–2005). GRACE TWS from the CSR datacenter is shown for the period 2002 to 2005 (green lines). Additionally, ERS SWI data (red lines) are shown for months with more than 50% areal coverage of the basin. The good agreement between GRACE and EI-BSWB TWS found in Figure 5 can also be seen in Figure 6: The TWS from the two datasets have

Table III. Correlations between TWS and SWI anomalies from different datasets for the given number of common observations (n_obs)

		EI-BSWB with E40-BSWB	n_obs	EI-BSWB with GSWP	n_obs	EI-BSWB with GRACE	n_obs	EI-BSWB with ERS	n_obs	Basin size [km ²]
1	Weser	0.60	124	0.61	66	—	2	0.41	63	35 888
2	Garonne	0.62	128	0.52	66	−0.10	43	0.24	134	49 381
3	Ebro	−0.72	12	0.57	57	—	0	0.36	99	83 930
4	Seine	0.56	128	0.41	66	0.77	22	0.55	102	84 144
5	Po	—	1	0.05	36	0.47	43	0.47	38	85 223
6	Rhone	0.35	128	0.44	66	0.42	20	0.32	97	94 836
7	Loire	0.58	128	0.63	66	0.14	43	0.42	132	107 646
8	Odra	−0.27	34	0.67	66	0.24	43	0.36	87	107 992
9	Elbe	0.76	128	0.79	66	0.59	43	0.38	74	132 014
10	Rhine	0.55	128	0.76	66	0.55	43	0.20	78	160 704
11	Syrdarya	0.73	21	−0.53	21	—	0	—	0	166 381
12	Wisla	0.44	34	0.31	34	—	0	0.31	7	193 500
13	Illinois	0.88	128	0.69	66	0.18	41	0.10	101	203 549
14	Amudarya	0.53	21	0.52	66	0.58	43	0.35	57	321 599
15	French basins	0.63	128	0.59	66	0.05	21	0.44	102	336 007
16	Arkansas	0.65	128	0.55	66	0.25	41	0.36	120	382 423
17	Ohio	0.70	128	0.61	66	−0.31	41	0.03	116	503 558
18	Columbia	0.82	108	0.68	66	0.35	41	−0.05	71	503 558
19	Danube	0.78	96	0.40	66	—	0	0.28	55	772 220
20	Yukon	0.83	48	0.25	57	0.16	40	0.30	19	779 081
21	Changjiang	0.84	128	0.56	66	0.28	43	0.15	98	965 180
22	Murray-Darling	0.81	128	0.84	66	0.28	43	0.53	112	1006 173
23	Missouri	0.89	128	0.71	66	0.36	43	0.60	84	1 201 513
24	Volga	0.91	92	0.68	30	—	0	0.71	54	1 333 747
25	Mackenzie	0.95	60	0.70	66	−0.31	10	0.46	47	1 587 878
26	Amur	—	0	—	0	0.41	32	—	0	1 921 624
27	Lena	0.90	128	0.38	66	—	0	0.10	42	2 351 052
28	Yenisei	0.97	128	0.69	66	0.66	10	0.15	53	2 513 361
29	Ob	0.96	96	0.82	66	—	0	0.42	37	2 859 889
30	Mississippi	0.89	72	0.82	66	0.64	11	0.55	36	2 868 901

For TU Wien ERS data, only months with more than 50% of basin area covered are considered. Correlations significant on a 95% level are displayed in bold face.

similar seasonal cycles in the overlapping years 2002 to 2005. ERS SWI data show striking similarities to BSWB TWS over the whole available period. For example in the Murray-Darling basin, many water storage peaks such as e.g. in August 1996 and 1998, are captured well regarding timing and amplitude.

Table III displays the correlations of the anomalies of the EI-BSWB dataset with the E40-BSWB, GSWP, GRACE, and ERS datasets. The numbers of mutual observations are also provided. Values significant on a 95% level are displayed in bold face. In most basins, highly significant correlations between the EI-BSWB and the GSWP data are found. As expected given the low resolution of GRACE, ERS data show higher correlations with the EI-BSWB dataset in small river basins. Nevertheless, also GRACE estimates show promising high correlations in many basins. It is known that scatterometer measurements are generally not reliable in desert, high-latitude, and mountain areas (Wagner *et al.* 2003, de Jeu *et al.* 2008). This is supported by the small correlation between ERS and EI-BSWB data in the Rhine river basin, where GRACE in contrast shows very good agreement with the EI-BSWB data. Interestingly, in the Ohio basin, the agreement of the two satellite derived datasets

with BSWB data is low, whereas they agree quite well with one another (see also Figure 3, right column third panel from top). This indicates a deficiency of the EI-BSWB data in the Ohio basin, which is supported by the relatively large imbalance for this basin compared to its size (Table II). This was not the case in the previously derived E40-BSWB dataset, as seen in Figure 2 (basin size of about 500 000 km²). Possible causes for this difference should be investigated.

For a geographical overview, Figure 3 displays the anomaly correlations of the TWSC from EI-, E40-BSWB, GSWP, GRACE, and ERS. Basins where the correlations are based on less than 30 data pairs are hatched. Note that in the smaller European basins, GRACE and ERS data generally compare less well with EI-BSWB than GSWP. In larger basins, also the satellite retrievals compare well to the BSWB estimates.

In Figure 7, TWSC from the EI- and E40-BSWB and GSWP model output are compared to *in situ* observations in the Ob basin and Illinois. The number of observations used for the calculation of the correlations is displayed in the figure. In both basins, the correlation to observations is higher in the EI- than in the E40-BSWB data. In Illinois, the GSWP data compares best to the observations,

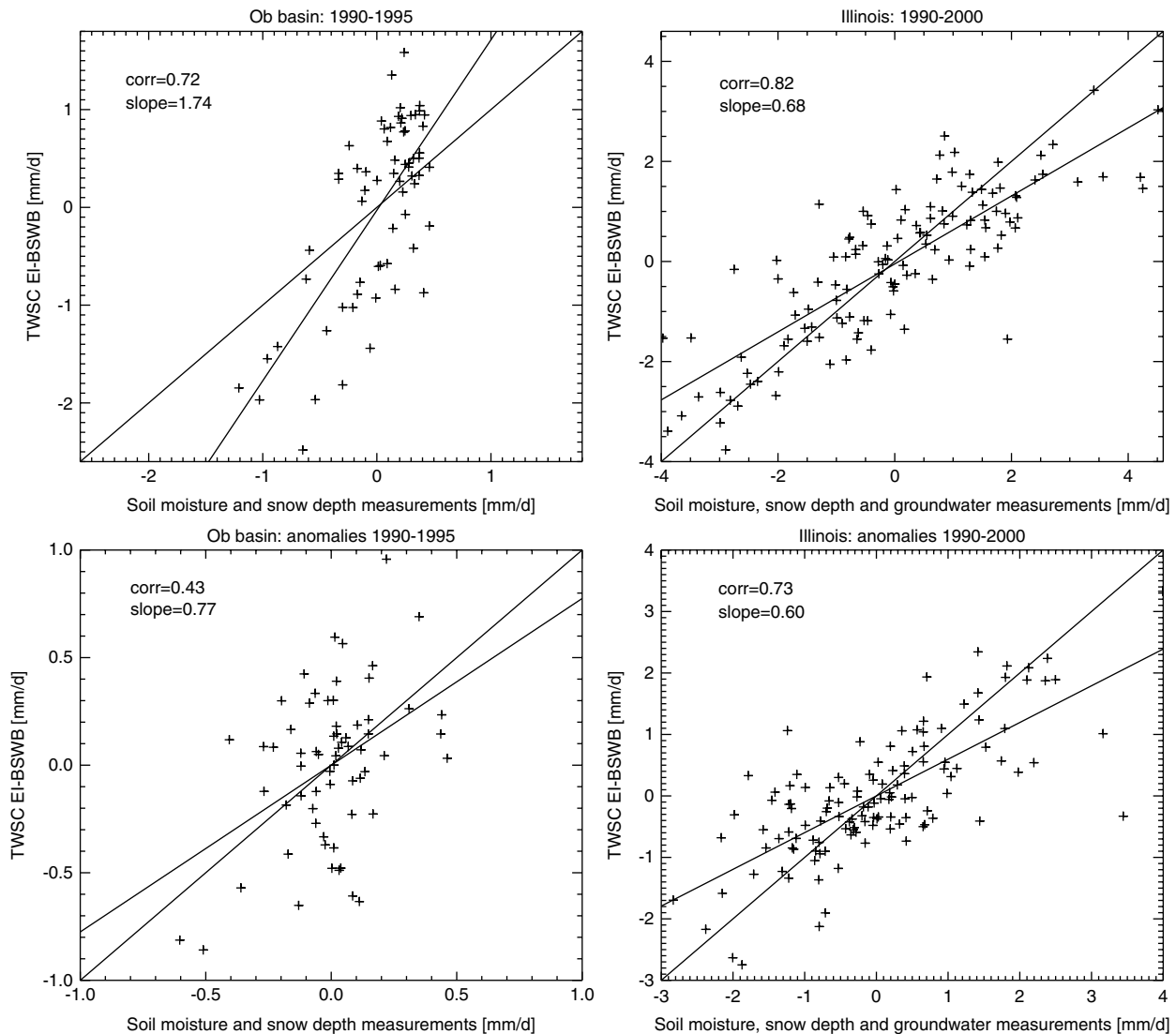


Figure 4. Scatter diagram of EI-BSWB estimates and *in situ* observations of soil moisture and snow depth in the Ob river basin and soil moisture, snow depth, and groundwater in Illinois (top TWSC, bottom TWSC anomalies, i.e. removed seasonal cycle)

whereas in the Ob basin, both the EI- and E40-BSWB estimates agree better with the observations than GSWP.

SUMMARY AND CONCLUSIONS

The new ECMWF reanalysis ERA-Interim has been used to derive atmospheric-terrestrial water-balance estimates of TWSC for several river basins of the world. The new dataset (EI-BSWB) complements previous datasets derived from the ERA-40 reanalysis (E40-BSWB) and the ECMWF operational forecast analysis data. This study focused on the evaluation of the newly derived dataset and on the quantification of uncertainty estimates for the BSWB approach.

The main source of uncertainty was found in the moisture convergence. In many river basins, it contributes to more than 80% of the total estimated uncertainty. The relative estimated uncertainty of the BSWB data is less than 10% of the mean annual amplitude in the largest basins under consideration, but can be quite important

in small basins. The imbalances between the employed atmospheric (moisture flux convergence) and terrestrial (streamflow measurement) data show large variations between the considered river basins. They are generally smaller in large basins. Compared with the previously derived E40-BSWB data (Hirschi *et al.* 2006a), the imbalances in many basins changed from a positive to a negative sign in the new EI-BSWB dataset. This means that in these basins, the values of moisture flux convergence or total column water vapour are smaller in ERA-Interim than ERA-40. The total and relative estimated uncertainties calculated from the differences between the ERA-Interim and ERA-40 (ERA-Interim reanalysis and 6-h forecast, respectively) moisture flux convergence fields are larger than the imbalances in all the basins except for the Murray-Darling basin (and the Ohio and Yenisei basins, respectively).

We further conducted a comparison of BSWB, GRACE, ERS, and GSWP data. The EI-BSWB and ERS data compare well despite their differences in spatial resolution and definition of water storage (the ERS data does

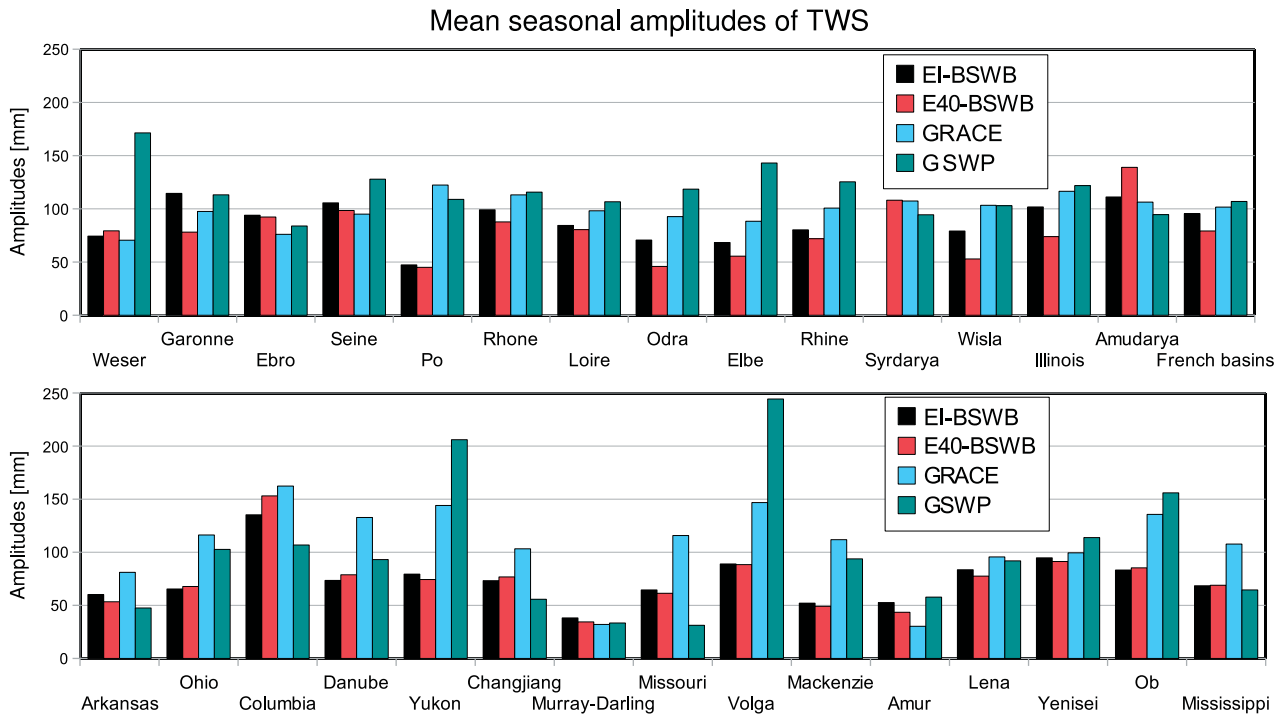


Figure 5. Comparison of mean seasonal amplitudes of EI- (black), E40-BSWB (red), GRACE (blue) and GSWP (turquoise) TWS over the period of available data (at least 24 months)

not include ground and surface water). The correlations of their anomalies are highly significant in nearly all basins. The employed GRACE data compares less well to EI-BSWB, but still has significant correlations in 10 out of

the 22 basins with overlapping years. The GSWP and EI-BSWB datasets agree well.

In conclusion, BSWB estimates derived from ERA-Interim reanalysis and measured streamflow are found to

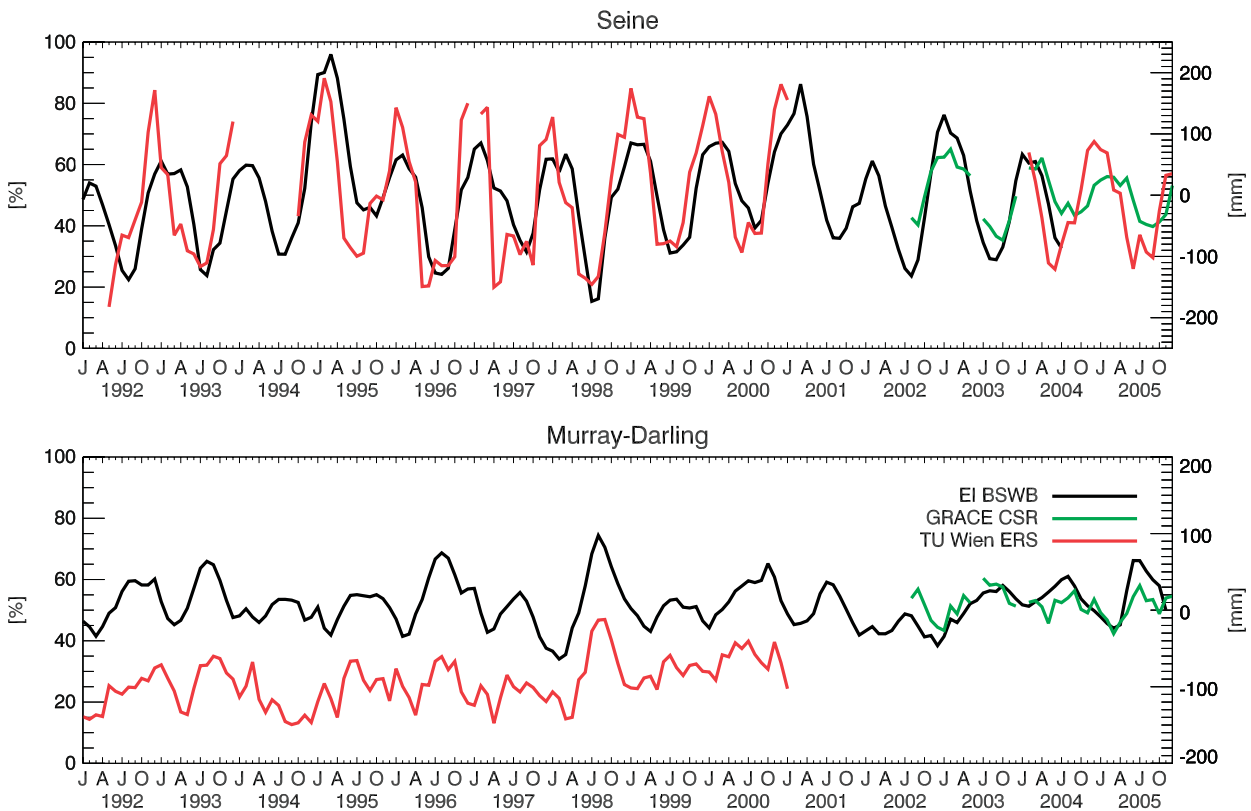


Figure 6. TWS in the Seine (upper graph) and the Murray-Darling (lower graph) river basins, from January 1992 to December 2005. TU Wien ERS data are considered when more than 50% of the area is covered. Note the different axes on the left (%) for ERS SWI and on the right (mm) for BSWB and GRACE TWS

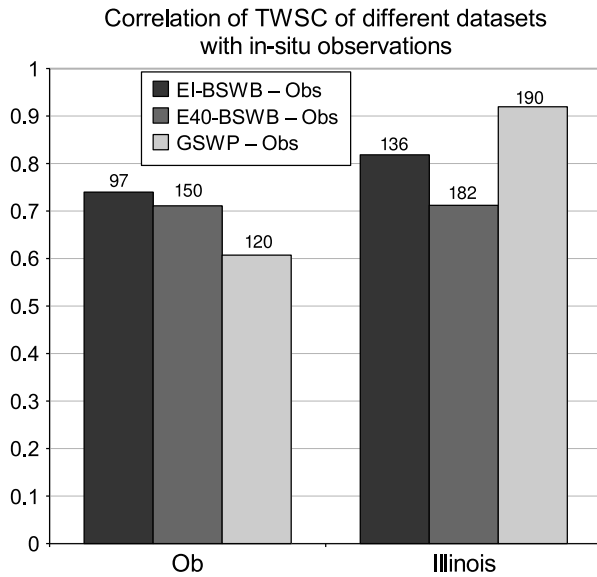


Figure 7. Correlations of TWSC from EI-BSWB, E40-BSWB, and GSWP to *in situ* observations (Obs). The observation data period is 1986–2001 for Illinois, and 1986–1998 for the Ob basin. The actual number of data points used for the computation of the correlation is displayed on top of each column. In the Ob basin, snow observations are only included before 1995

provide accurate estimates of TWSC. Satellite retrievals from ERS, which have a resolution of 25 km, agree very well with these estimates. GRACE satellites retrievals compare less well in small basins, which might be due to their coarse resolution (500 km). Real-time BSWB estimates of TWSC based on ERA-Interim can be derived in most large river basins where streamflow measurements are available. This is of strong relevance for several agricultural, hydrological, and climate applications given the importance of TWSC for society.

ACKNOWLEDGEMENTS

Divergence of water vapour fields (ERA-Interim reanalysis and 6-h forecast, and ERA-40) were kindly computed at the ECMWF by Dr Gianpaolo Balsamo. We are also most grateful for his comments on this study.

We would also like to thank all the providers of streamflow data: The GRDC team in Koblenz (Germany), the USGS team, the U.S. Army, the R-Arctic net team and Dr Alexander Shiklomanov from the University of New Hampshire (USA), Prof. V.E. Chub from the Centre of Hydrometeorological Service, Tashkent (Republic of Uzbekistan), Dr Yusup Khaidarovich Rysbekov from the ICWC of Central Asia, Tashkent (Republic of Uzbekistan), the Surface Water Archive team of the Government of South Australia (AUS), Nicolas THEVENET from the Compagnie Nationale du Rhône (France), Dr Hessel C. Winsemius from the TUDelft (Netherlands), Martina Mildner from the Wasser- und Schifffahrtsamt Verden (Germany), the team of the Cofederacion Hidrografica del Ebro (Spain), Boguslaw Tadeuszewski from the Instytut Meteorologii i Gospodarki Wodnej, Warszawa (Poland).

We would like to thank the Global Soil Moisture Data Bank team for access to soil water validation data.

REFERENCES

- Andersen OB, Seneviratne SI, Hinderer J, Viterbo P. 2005. GRACE-derived terrestrial water storage depletion associated with the 2003 European heat wave. *Geophysical Research Letters* **32**(18): L18405. DOI: 10.1029/2005GL023574.
- Awange JL, Sharifi MA, Baur O, Keller W, Featherstone WE, Kuhn M. 2009. GRACE hydrological monitoring of Australia: current limitations and future prospects. *Journal of Spatial Science* **54**(1): 23–36.
- Balsamo G, Viterbo P, Beljaars A, van den Hurk B, Hirschi M, Betts AK, Scipal K. 2009. A revised hydrology for the ECMWF model: verification from field site to terrestrial water storage and impact in the integrated forecast system. *Journal of Hydrometeorology* **10**(3): 623–643. DOI: 10.1175/2008JHM1068.1.
- Berbery EH, Rasmusson EM. 1999. Mississippi moisture budgets on regional scales. *Monthly Weather Review* **127**(11): 2654–2673.
- Bettadpur S. 2007. Gravity recovery and climate experiment product specification document. Technical Report (Rev 4.5, February 20, 2007, 1–77), Center for Space Research, The University of Texas at Austin.
- Dirmeyer PA, Gao XA, Zhao M, Guo ZC, Oki TK, Hanasaki N. 2006. GSWP-2—multimodel analysis and implications for our perception of the land surface. *Bulletin of the American Meteorological Society* **87**(10): 1381–1397.
- Draper C, Mills G. 2008. The atmospheric water balance over the semiarid Murray-Darling river basin. *Journal of Hydrometeorology* **9**(3): 521–534. DOI: 10.1175/2007JHM889.1.
- Fitzmaurice J, Bras RL. 2008. Comparing reanalyses using analysis increment statistics. *Journal of Hydrometeorology* **9**(6): 1535–1545. DOI: 10.1175/2008JHM946.1.
- Guo ZC, Dirmeyer PA, Gao X, Zhao M. 2007. Improving the quality of simulated soil moisture with a multi-model ensemble approach. *Quarterly Journal of Royal Meteorological Society* **133**(624): 731–747.
- Gutowski WJ, Chen Y, Ötles Z. 1997. Atmospheric water vapor transport in NCEP-NCAR reanalyses: comparison with river discharge in the Central United States. *Bulletin of the American Meteorological Society* **78**(9): 1957–1969. DOI: 10.1175/1520-0477(1997)078<1957:AWVTIN>2.0.CO;2.
- Hirschi M, Seneviratne SI, Hagemann S, Schär C. 2007. Analysis of seasonal simulated water storage variations in regional climate simulations over Europe. *Journal of Geophysical Research-Atmospheres* **112**(D22): D22109. DOI: 10.1029/2006JD008338.
- Hirschi M, Seneviratne SI, Schär C. 2006a. Seasonal variations in terrestrial water storage for major midlatitude river basins. *Journal of Hydrometeorology* **7**(1): 39–60.
- Hirschi M, Viterbo P, Seneviratne SI. 2006b. Basin-scale water-balance estimates of terrestrial water storage variations from ECMWF operational forecast analysis. *Geophysical Research Letters* **33**: L21401, DOI: 10.1029/2006GL027659.
- Jaeger EB, Stockli R, Seneviratne SI. 2009. Analysis of planetary boundary layer fluxes and land-atmosphere coupling in the regional climate model CLM. *Journal of Geophysical Research-Atmospheres* **114**: D17106, pp.1–15. DOI: 10.1029/2008JD011658.
- de Jeu RAM, Wagner W, Holmes TRH, Dolman AJ, van de Giesen NC, Friesen J. 2008. Global soil moisture patterns observed by space borne microwave radiometers and scatterometers. *Survey of Geophysics* **29**: 399–420. DOI:10.1007/s10712-008-9044-0.
- Kleidon A, Heimann M. 2000. Assessing the role of deep rooted vegetation in the climate system with model simulations: mechanism, comparison to observations and implications for Amazonian deforestation. *Climate Dynamics* **16**(2–3): 183–199. DOI: 10.1007/s003820050012.
- Koster RD, Dirmeyer PA, Guo ZC, Bonan G, Chan E, Cox P, Gordon CT, Kanae S, Kowalczyk E, Lawrence D, Liu P, Lu CH, Malyshev S, McAvaney B, Mitchell K, Mocko D, Oki T, Oleson K, Pitman A, Sud YC, Taylor CM, Verseghy D, Vasic R, Xue YK, Yamada T. 2004. Regions of strong coupling between soil moisture and precipitation. *Science* **305**(5687): 1138–1140.
- Masuda K, Hashimoto Y, Matsuyama H, Oki T. 2001. Seasonal cycle of water storage in major river basins of the world. *Geophysical Research Letters* **28**(16): 3215–3218.
- McCabe MF, Wood EF, Wojcik R, Pan M, Sheffield J, Gao H, Su H. 2008. Hydrological consistency using multi-sensor remote sensing data for water and energy cycle studies. *Remote Sensing of Environment* **112**(2): 430–444. DOI: 10.1016/j.rse.2007.03.027.

- Ramillien G, Famiglietti JS, Wahr J. 2008. Detection of continental hydrology and glaciology signals from GRACE: a review. *Survey of Geophysics* **29**(4–5): 361–374. DOI: 10.1007/s10712-008-9048-9.
- Rasmusson EM. 1968. Atmospheric water vapor transport and the water balance of North America. *Monthly Weather Review* **96**(10): 720–734.
- Robock A, Vinnikov KY, Srinivasan G, Entin JK, Hollinger SE, Speranskaya NA, Liu SX, Namkhai A. 2000. The global soil moisture data bank. *Bulletin of the American Meteorological Society* **81**(6): 1281–1299.
- Rodell M, Famiglietti JS, Chen J, Seneviratne SI, Viterbo P, Holl S, Wilson CR. 2004. Basin scale estimates of evapotranspiration using GRACE and other observations. *Geophysical Research Letters* **31**(20): L20504.
- Rodell M, Velicogna I, Famiglietti JS. 2009. Satellite-based estimates of groundwater depletion in India. *Nature* **460**(7258): 999–1002. DOI: 10.1038/nature08238.
- Scipal K, Wagner W, Trommler M, Naumann K. 2002. The global soil moisture archive 1992–2000 from ERS scatterometer data: first results. *Proceedings of IEEE International Geoscience and Remote Sensing Symposium*. IEEE: Piscataway, NJ.
- Seneviratne SI, Corti T, Davin EL, Hirschi M, Jaeger EB, Lehner I, Orlowsky B, Teuling AJ. 2010. Investigating soil moisture-climate interactions in a changing climate: a review. *Earth Science Reviews* DOI: 10.1016/j.earscirev.2010.02.004.
- Seneviratne SI, Koster RD, Guo ZC, Dirmeyer PA, Kowalczyk E, Lawrence D, Liu P, Lu CH, Mocko D, Oleson KW, Verseghy D. 2006a. Soil moisture memory in AGCM simulations: analysis of global land-atmosphere coupling experiment (GLACE) data. *Journal of Hydrometeorology* **7**(5): 1090–1112.
- Seneviratne SI, Lüthi D, Litschi M, Schär C. 2006b. Land-atmosphere coupling and climate change in Europe. *Nature* **443**(7108): 205–209.
- Seneviratne SI, Viterbo P, Lüthi D, Schär C. 2004. Inferring changes in terrestrial water storage using ERA-40 reanalysis data: The Mississippi river basin. *Journal of climate* **17**(11): 2039–2057.
- Simmons AJ, Uppala SM, Dee D, Kobayashi S. 2006/2007. ERA-Interim: new ECMWF reanalysis products from 1989 onwards. ECMWF News letter No. 110, pp. 25–35.
- Swenson S, Yeh PJF, Wahr J, Famiglietti J. 2006. A comparison of terrestrial water storage variations from GRACE with in situ measurements from Illinois. *Geophysical Research Letters* **33**(16): L16401. DOI: 10.1029/2006GL026962.
- Syed TH, Famiglietti JS, Chen J, Rodell M, Seneviratne SI, Viterbo P, Wilson CR. 2005. Total basin discharge for the Amazon and Mississippi river basins from GRACE and a land-atmosphere water balance. *Geophysical Research Letters*, **32**: L24404, DOI:10.1029/2005GL024851.
- Trenberth KE, Smith L, Qian TT, Dai AG, Fasullo J. 2007. Estimates of the global water budget and its annual cycle using observational and model data. *Journal of Hydrometeorology* **8**(4): 758–769. DOI: 10.1175/JHM600.1.
- Troch P, Durcik M, Seneviratne SI, Hirschi M, Teuling AJ, Hurkmans R, Hasan S. 2007. New data sets to estimate terrestrial water storage change. *Eos Transactions, AGU* **88**(45): 469–470.
- Uppala SM, Kallberg PW, Simmons AJ, Andrae U, Bechtold VD, Fiorino M, Gibson JK, Haseler J, Hernandez A, Kelly GA, Li X, Onogi K, Saarinen S, Sokka N, Allan RP, Andersson E, Arpe K, Balmaseda MA, Beljaars ACM, Van De Berg L, Bidlot J, Bormann N, Caires S, Chevallier F, Dethof A, Dragosavac M, Fisher M, Fuentes M, Hagemann S, Holm E, Hoskins BJ, Isaksen L, Janssen PAEM, Jenne R, McNally AP, Mahfouf JF, Morcrette JJ, Rayner NA, Saunders RW, Simon P, Sterl A, Trenberth KE, Untch A, Vasiljevic D, Viterbo P, Woollen J. 2005. The ERA-40 re-analysis. *Quarterly Journal of Royal Meteorological Society* **131**(612): 2961–3012.
- Wagner W, Scipal K, Pathe C, Gerten D, Lucht W, Rudolf B. 2003. Evaluation of the agreement between the first global remotely sensed soil moisture data with model and precipitation data. *Journal of geophysical research* **108**(D19): 4611. DOI: 10.1029/2003JD003663.
- Yamamoto K, Fukuda Y, Nakaegawa T, Nishijima J. 2007. Landwater variation in four major river basins of the Indochina peninsula as revealed by GRACE. *Earth, Planets and Space* **4**(4): 193–200.
- Yeh PJF, Irizarry M, Eltahir EAB. 1998. Hydroclimatology of Illinois: a comparison of monthly evaporation estimates based on atmospheric water balance and soil water balance. *Journal of Geophysical Research-Atmospheres* **103**(D16): 19823–19837.
- Zeng N, Yoon JH, Mariotti A, Swenson S. 2008. Variability of basin-scale terrestrial water storage from a PER water budget method: the Amazon and the Mississippi. *Journal of climate* **21**(2): 248–265. DOI: 10.1175/2007JCLI1639.1.